Copyright © 2014 Tech Science Press CMC, vol.42, no.3, pp.175-203, 2014

From Geometric Transformations to Auxetic Metamaterials

Ligia Munteanu[1], Veturia Chiroiu[1] and Viorel Şerban[2]

Abstract: The paper introduces a new alternative towards fabrication of auxetic metamaterials (materials with negative Poisson's ratio) controlled by geometric transformations. These transformations are derived from the theory of small (infinitesimal) elastic deformation superimposed on finite elastic deformations. By using this theory, a cylindrical region filled with initial deformed foam is transformed through deformation into a cylindrical shell region filled with auxetic metamaterial. As an example, the realization of the seismic cloak device becomes a practical possibility.

Keywords: Geometric transformation, Auxetic metamaterial, Seismic cloak.

1 Introduction

The primary aim of this paper is to discuss the auxetic metamaterials controlled by geometric transformations. These geometric transformation are derived from the theory of small (infinitesimal) elastic deformation superimposed on finite elastic deformations [Toupin and Bernstein (1961); Bradford and Pi (2012)]. This theory is used for describing the deformation of a cylindrical region filled with initial deformed foam. Finally, a cylindrical shell region filled with auxetic metamaterial is obtained. Auxetic behavior (negative Poisson ratio) exists across an enormous range of conditions, from near absolute zero and densities of approximately 10^{-15}gcm^{-3} for plasma ion crystals to above 10^{6}K and densities of 10^{11}gcm^{-3} for crystals [Baughman (2003); Lakes (1986, 1987, 1991)]. The term *auxetic* is coming from the Greek word *auxetos*, meaning *that which may be increased*. The direct effect of a negative Poisson's ratio is to cause an expansion that decreases density during streching. Baughman and Galvao (1993) have found a negative Poisson's ratio in cubic crystals when they are stretched along the [110] and $[1\bar{1}0]$ direction.

[1] Institute of Solid Mechanics, Romanian Academy, Ctin Mille 15, 010141Bucharest, Romania. E-mails: ligia_munteanu@hotmail.com; veturiachiroiu@yahoo.com

[2] Subsidiary of Technology and Engineering for Nuclear Projects, Atomistilor Street 409, Magurele, Bucharest. E-mail: office@serb.ro

Auxetic materials with lower symmetry can have giant strain amplification factors in comparison with the non-auxetic ones [Lakes and Elms (1993); Scarpa et al. (2005); Bezazi and Scarpa (2007); Donescu et al. (2009); Munteanu et al. (2012)]. However, auxetic materials can have a Poisson's ratio about 40 times larger than that for most materials; for example the porous polytetrafluoroethylene has a Poisson's ratio up to -12 [Baughman (2003)].

In addition to traditional auxetic materials, auxetic metamaterials undergoe enormous flexibility and sustain a wide range of deformations which vary at different frequencies. Their buckling makes no much difference between 1kHz (λ =300km) and 1THz (λ=0.3mm). The structure of auxetic metamaterials is atomic and the arrangement of meta-cell is about 10^{-10}m, just as required for seismic cloaking [Chiroiu et al. (2014)]. The problem is related to the current research in invisibility cloaks via geometric transformations [Milton (2007); Milton and Nicorovici (2006); Schurig, Pendry and Smith (2006); Munteanu and Chiroiu (2011); Munteanu (2012)] and sonic composites [Hirsekorn et al. (2004); Munteanu and Chiroiu (2010); Choudhury and Iha (2013); Chiroiu et al. (2013); Munteanu et al. (2014)].

Pendry et al (2006) and Leonhardt (2006) deduced from a geometric transformation in the Maxwell system a cloak that renders any object inside it invisible to electromagnetic radiation.

In acoustics, the idea of the invisibility cloak is that the sound sees the space differently [Dupont et al. (2011); Qiu et al. (2009)]. Cummer and Schurig (2007) analyzed a 2D acoustic cloaking for pressure waves in a transversely anisotropic fluid, while Novitsky et al. (2009) proposed a method for spherical invisibility cloaks, in which we do not need to know or use the coordinate transformation. By virtue of the cloak-generating function, all the parameters of the radially anisotropic spherical cloak are determined analytically and uniquely.

Norris (2008) presented a theory of transformation acoustics that enables the realization of pentamode acoustic materials having anisotropic density and finite mass. This theory permits considerable freedom in choosing the transformation from physical to virtual space. Scandrett, Boisvert and Howarth (2010) extended this work by considering a range of cloaks, from those comprised of fluid layers which are isotropic in bulk moduli with anisotropic density to those having anisotropic bulk moduli and isotropic density.

Starting from the same work, Cipolla, Gokhale and Norris (2010) investigate 3D acoustic materials composed of combinations of simple geometric shapes, e.g., a cylinder with spherical end-caps. Certain classes of transformations for the design of such shapes are described and also, conditions under which these transforma-

tions result in materials which minimize acoustic reflections. The standard process for defining cloak materials is to first define the transformation and then evaluate whether the materials are practically realizable. The same authors, Cipolla, Gokhale and Norris (2012) have inverted this process by defining desirable material properties and then deriving the appropriate transformations which guarantee the cloaking effect.

Another approach is to develop materials with normal elastic behavior that approximate the Cosserat material [Cosserat and Cosserat (1909)]. Preliminary work in this direction has been considered by Norris and Shuvalov (2011). The general theory has been applied to the case of cylindrical anisotropy for arbitrary radial transformation.

The equations of motion for the transformed Cosserat material have been expressed in Stroh format, suitable for modeling cylindrical elastic cloaking. It is shown that there is a preferred approximate material with symmetric stress that could be a useful candidate for making cylindrical elastic cloaking devices.

Parnell (2012) has shown that cloaking of objects from antiplane elastic waves can be achieved by employing nonlinear elastic pre-stress in a neo-Hookean elastomeric material. This approach would appear to eliminate the requirement of metamaterials with inhomogeneous anisotropic shear moduli and density. Waves in the pre-stressed medium are bent around the cloaked (cavity) region by inducing inhomogeneous stress fields via pre-stress. The equation governing antiplane waves in the pre-stressed medium is equivalent to the antiplane equation in an unstressed medium with inhomogeneous and anisotropic shear modulus and isotropic scalar mass density.

Transformation elasticity, by analogy with transformation acoustics and optics, converts material domains without altering the wave properties. Milton and Cherkaev addressed in 1995 the following question: *What are possible elasticity tensors of anisotropic materials*? The answer is based on the arguments that any positive-definite tensor can be realized as the effective elasticity tensor. So far, pentamodes proposed by Milton and Cherkaev have been purely theoretical. The word *penta* is derived from ancient Greek and means *five*. In the case of water, the five shear parameters equal zero, and only one parameter, compression, differs from that value. Following this theory Kadic et al. (2012) and Bückmann et al. (2012) have investigated and fabricated pentamode metamaterials by optical lithography. More recently, a elastostatic cloak was made by Wegener's group for pentamode materials. Intensive work was made by the same group to try to control all quantities that usually characterise the mechanical materials [Stenger, Wilhelm and Wegener (2012); Kadic et al. (2012)]. A multilayered radar absorbing structure (RAS) has been presented by Narayan, Latha and Jha (2013) based on transmission

line transfer matrix method for millimeter wave applications.

Geometric transformations cannot be applied to equations which are not invariant under coordinate transformations and, consequently, if cloaking exists for such equations (for example the elasticity equations), it would be of a different nature from acoustic and electromagnetic [Milton, Briane and Willis (2006)]. The existence of an acoustic cloaking indicates that cloaks might possibly be built for other wave systems, including seismic waves that travel through the earth and the waves at the surface of the ocean [Cummer et al. (2008)]. Farhat et al. (2009) discussed a special case of thin-elastic plates, for which the elasticity tensor is represented in a cylindrical basis by a diagonal matrix with two (spatially varying) non-vanishing entries. In a similar manner, Brun et al. (2009) derived the elastic properties of a cylindrical cloak for in-plane coupled shear and pressure waves.

So, the following question arises: *What kind of geometric transformations can be used for controlling elastic wave?* To answer this question, we will reconsider the transformation itself and examine how the field and material are transported to a new compressed space, by using the theory of small (infinitesimal) elastic deformation superimposed on finite elastic deformations [Toupin and Bernstein (1961)].

In this paper, the theory of small (infinitesimal) elastic deformation superimposed on finite elastic deformations is applied to deform a cylindrical region $r \leq R_2$ filled with initial deformed foam in the original space Ω into a cylindrical shell region $R_1 \leq r' \leq R_2$ filled with auxetic metamaterial in the compressed space Ω'. In the original and final domains, the outer radius R_2 is fixed.

The paper is organized as follows: Section 2 is devoted to geometric transformations derived from the theory of small (infinitesimal) elastic deformation superimposed on finite elastic deformations. In Section 3, equations of motion for conventional foams are derived, and in Section 4 the transformed relations are developed. Section 5 is devoted to calculation of the material constants. The Lamé functions behavior is explained through the *crazing phenomenon* which is a failure mode met at the bulk polymers. The Section 6 is devoted to seismic cloaking. Buildings and foundations can be protected from earthquakes by surrounding them with special designed shells made of auxetic material. Conclusions are found in Section 7.

2 Geometric transformations

Let us consider the geometric transformation (pull-back) from the stretched coordinate system (x', y', z') of the compressed space to the original coordinate system (x, y, z), given by $x(x', y', z')$, $y(x', y', z')$ and $z(x', y', z')$. The change of coordinates is characterized by the transformation of the differentials through the Jacobian $J_{xx'}$

of this transformation, i.e.

$$\begin{pmatrix} \mathrm{d}x \\ \mathrm{d}y \\ \mathrm{d}z \end{pmatrix} = J_{xx'} \begin{pmatrix} \mathrm{d}x' \\ \mathrm{d}y' \\ \mathrm{d}z' \end{pmatrix}, \quad J_{xx'} = \frac{\partial(x,y,z)}{\partial(x',y',z')}. \tag{1}$$

From the geometrical point of view, the change of coordinates implies that, in the transformed region, one can work with an associated metric tensor [Zolla et al. (2007); Guenneau et al. (2011); Nicorovici (1994);Torrent and Sánchez-Dehesa (2008)]

$$T = \frac{J_{xx'}^T J_{xx'}}{\det(J_{xx'})}. \tag{2}$$

In terms of the acoustic parameters, one can replace the material from the original domain (homogeneous and isotropic) by an equivalent compressed one that is inhomogeneous (its characteristics depend on the (x',y',z') coordinates) and anisotropic (described by a tensor), and whose properties, in terms of $J_{x'x}$, are given by

$$\rho' = J_{x'x}^{-\mathrm{T}} \cdot \rho \cdot J_{x'x}^{-1} \cdot \det(J_{x'x}), \quad \kappa' = \kappa \det(J_{x'x}), \tag{3}$$

or, equivalently, in terms of $J_{xx'}$

$$\rho' = \frac{J_{xx'}^T \cdot \rho \cdot J_{x'x}}{\det(J_{xx'})}, \quad \kappa' = \frac{\kappa}{\det(J_{xx'})}. \tag{4}$$

Here, ρ' is a second order tensor. When the Jacobian matrix is diagonal, (3) and (4) can be more easily written. The cloak properties in transformed coordinates are given by (4) where $J_{r'r} = \partial r'/\partial r$.

The mapping given by (1) can be interpreted as a deformation applied to the initial space Ω in order to obtain the deformed space Ω'. In other words, a point and its infinitesimal region in Ω' is obtained from an affine deformation applied to an initial point and its infinitesimal region in Ω.

The theory of small (infinitesimal) elastic deformation superimposed on finite elastic deformations given by Toupin and Bernstein in 1961 is used to deform a cylindrical region $r \leq R_2$ filled with traditional foam in the original space Ω into a cylindrical shell region $R_1 \leq r' \leq R_2$ filled with auxetic metamaterial in the compressed space Ω'. In the original and final domains, the outer radius R_2 is fixed.

To develop such a map, three simultaneously distinct configurations of the material points with the same origin O are introduced:

- natural or stress-free configuration C_0 (position of a point P has coordinates $\xi_\mu(\mathrm{P})$),

- initially deformed equilibrium configuration $\tilde{C}$ (position of a point P has coordinates $X_A(P)$),

- present configuration $C(t)$, where t is the time (position of a point P has coordinates x_i(P,t).

A motion of the material body is one parameter family of mappings

$$x_i = x_i(\xi, t), \quad \xi_\mu = \xi_\mu(x,t), \tag{5}$$

giving for each time t, a one-to-one relation between the present coordinates and the natural coordinates of each material point. The initial configuration is the present configuration at some time$t$, so that knowing the relation between the coordinate systems, we may deduce from (5) relations of the form

$$X_A = X_A(\xi), \quad \xi_\mu = \xi_\mu(X), \quad x_i = x_i(X,t), \quad X_A = X_A(x,t). \tag{6}$$

The equations of the theory of small deformations superimposed on an initial finite deformation are derived from the general equations of the homogeneous elastic materials

$$t_{ij,j} = \rho \ddot{x}_i, \tag{7}$$

$$t_{ij} = t_{ji} = \left(\frac{x}{\xi}\right)^{-1} \frac{\partial W(E)}{\partial E_{mn}} \frac{\partial x_i}{\partial \xi_\mu} \frac{\partial x_j}{\partial \xi_\nu},$$

$$t_{ij} = 0 \quad \text{if} \quad E_{\mu\nu} = 0,$$

$$\ddot{x}_i = \frac{\partial \dot{x}_i}{\partial t} + \dot{x}_{i,j}\dot{x}_j, \quad \dot{x}_i = \frac{\partial x_i(\xi,t)}{\partial t},$$

$$E_{\mu\nu} = \frac{1}{2}\left(\frac{\partial x_i}{\partial \xi_\mu}\frac{\partial x_i}{\partial \xi_\nu} - \delta_{\mu\nu}\right),$$

$$\rho = \rho_0 \left(\frac{x}{\xi}\right)^{-1}, \quad \rho_0 = \text{const.},$$

$$\left(\frac{x}{\xi}\right) \equiv \det\left(\frac{\partial x_i}{\partial \xi_\mu}\right).$$

In (5) we used the following notations:

t_{ij} components of the Cauchy stress tensor in $C(t)$,

ρ the present density of mass in $C(t)$,

ρ_0 the density of mass in the natural configuration C_0,

$\dot{x}_i$ components of the velocity vector,

$\ddot{x}_i$ components of the acceleration vector,

$\frac{\partial x_i}{\partial \xi_\mu}$ the deformation gradient of the present configuration relative to the natural configuration,

E_{mn} the set of six independent finite strain measures which vanish if and only if the motion from C_0 to $C(t)$ is rigid,

W is the stored elastic energy per unit underformed volume or elastic potential,

$\delta_{\mu\nu}$ the Christoffel symbol.

We assume that the elastic potential $W(E)$ is a polynomial in the finite strain measures

$$W(E) = \frac{1}{2} C_{\mu\nu\lambda\varsigma} E_{\mu\nu} E_{\lambda\varsigma}, \tag{8}$$

where $C_{\mu\nu\lambda\varsigma}$ are the second-order elastic constants.

We introduce the first order Piola-Kirchhoff non-symmetric stress tensor

$$\tau_{i\mu} = \left(\frac{x}{\xi}\right) \frac{\partial \xi_\mu}{\partial x_j} t_{ij}, \tag{9}$$

where $\frac{\partial \xi_\mu}{\partial x_j}$ is the inverse of $\frac{\partial x_j}{\partial \xi_\mu}$. The potential energy is given by

$$\bar{W}\left(\frac{\partial x_i}{\partial \xi_\mu}\right) = W(E), \tag{10}$$

since E is determined by $\frac{\partial x_i}{\partial \xi_\mu}$. We have

$$\tau_{i\mu} = \frac{\partial \bar{W}}{\partial\left(\frac{\partial x_i}{\partial \xi_\mu}\right)}. \tag{11}$$

Equations of motion $(7)_1$ may to transformed to

$$\tau_{i\mu,\mu} = \rho_0 \frac{\partial^2 x_i(\xi, t)}{\partial t^2}. \tag{12}$$

To obtain the equations of motion for a small deformation about the initial deformation, we consider the present coordinates $x_i(\mathrm{P})$ as functions $x_i(X_1, X_2, X_3, t)$ of the initial coordinates $X_A(\mathrm{P})$, in the present frame

$$x_i(X, t) = X_i + u_i(X, t), \tag{13}$$

where each component of the gradient $\frac{\partial u_i}{\partial X_j}$ of the displacement u_i of the present configuration relative to the initial configuration is small

$$\frac{\partial u_i}{\partial X_j} << 1 \quad \text{for} \quad t \geq \tilde{t}, \tag{14}$$

with $\tilde{t}$ time corresponding to the initial configuration. In other words, we assume that both the rotations and strains of the present configuration measured relative to the initial configuration remain small for all time after the initial configuration of the material points has been achieved. The functions $X_A(\xi)$ are satisfying the equilibrium equations corresponding to a biaxial deformation of the material

$$\tilde{\tau}_{i\mu,\mu} = 0, \quad \tilde{\tau}_{i\mu} = \frac{\partial \bar{W}}{\partial \left(\frac{\partial \tilde{x}_i}{\partial \xi_\mu} \right)}, \tag{15}$$

where $\frac{\partial \tilde{x}_i}{\partial \xi_\mu}$ is the deformation gradient in the initial configuration $\tilde{C}$.
The stress tensor $\tau_{i\mu}$ expands as follows

$$\tau_{i\mu} = \tilde{\tau}_{i\mu} + \frac{\partial^2 \bar{W}}{\partial \left(\frac{\partial \tilde{x}_i}{\partial \xi_\mu} \right) \partial \left(\frac{\partial \tilde{x}_k}{\partial \xi_\nu} \right)} u_{k;\nu} + \text{higher order terms in} \, (\text{grad}\, \mathbf{u}). \tag{16}$$

By setting

$$\tilde{\alpha}_{k\nu i\mu} = \tilde{\alpha}_{i\varpi k\nu} = \frac{\partial^2 \bar{W}}{\partial \left(\frac{\partial \tilde{x}_i}{\partial \xi_\mu} \right) \partial \left(\frac{\partial \tilde{x}_k}{\partial \xi_\nu} \right)}, \tag{17}$$

and using (15) we see from (12) that the linearized equations of motion for u_i have the form

$$(\tilde{\alpha}_{i\mu k\nu} u_{k,\theta})_{,\mu} = \rho_0 \frac{\partial^2 u_i}{\partial t^2}. \tag{18}$$

Eqs. (18) are the natural form of the motion equations. Eqs. (18) may to transform to the initial form of the equations of motion for small displacement u_i

$$(\tilde{A}_{iMkN} u_{k,N})_{,M} = \tilde{\rho} \frac{\partial^2 u_i}{\partial t^2} \tag{19}$$

where $\tilde{\rho} = \rho \left(\frac{x}{X} \right)^{-1}$ is the density of mass in the deformed configuration $\tilde{C}$, and

$$\tilde{A}_{iMkN} = \left(\frac{X}{\xi} \right)^{-1} \frac{\partial X_M}{\partial \xi_\mu} \frac{\partial X_N}{\partial \xi_\nu} \tilde{\alpha}_{i\mu k\nu} \quad . \tag{20}$$

3 Cosserat equations

The behavior of conventional foams is described by Cosserat theory [Cosserat and Cosserat (1909); Mindlin (1965); Gauthier (1982); Donescu et al. (2009)]. Chiral materials are not invariant to inversions: there is a distinction between right- and left-handed material [Lakes (1986, 1987, 1991)]. An elastic chiral material (noncentrosymmetric material) is isotropic with respect to coordinate rotations but not with respect to inversions. Chiral effects cannot be expressed within classical elasticity since the modulus tensor, which is fourth rank, is unchanged under an inversion

$$\begin{aligned} C_{ijkl} &= \frac{\mathrm{d}x_m}{\mathrm{d}x_i}\frac{\mathrm{d}x_n}{\mathrm{d}x_j}\frac{\mathrm{d}x_o}{\mathrm{d}x_k}\frac{\mathrm{d}x_p}{\mathrm{d}x_l}C_{mnop} \\ &= (-1)\delta_{im}(-1)\delta_{jn}(-1)\delta_{ok}(-1)\delta_{pl}C_{mnop} = (-1)^4 C_{ijkl} = C_{ijkl} \end{aligned} \tag{21}$$

Materials may exhibit chirality on the atomic scale, as in quartz, sugar and in biological molecules. Materials may also exhibit chirality on a larger scale, as in bones, porous materials, composites containing twisted or spiraling fibers, composites with helical or screw-shaped inclusions. Materials such as piezoelectrics, represented by tensors of fifth rank, are also chiral.

A chiral Cosserat material has three new elastic constants in addition to the six considered in the isotropic micropolar solid. Tensor properties of odd rank are zero if there is inversion symmetry, and can only be nonzero if there is handedness.

In the following we shortly present the theory of chiral Cosserat medium in the absence of body forces and body couples written in a Cartesian coordinates system (x_1, x_2, x_3) [Eringen (1966, 1968); Lakes and Benedict (1982)]. The motion equations are written as

$$\sigma_{kl,k} - \rho\ddot{u}_l = 0, \quad m_{rk,r} + \varepsilon_{klr}\sigma_{lr} - \rho j\ddot{\varphi}_k = 0, \tag{22}$$

where σ_{kl} is the stress tensor, m_{kl} is the couple stress tensor, u is the displacement vector, φ_k is the microrotation vector which in Cosserat elasticity is kinematically different from the macrorotation vector $r_k = \frac{1}{2}\varepsilon_{klm}u_{m,l}$, ρ is the mass density and j is the microinertia and ε_{klm} is the Levi-Civita permutation tensor. The quantities φ_k refers to the rotation of points themselves, while r_k refers to the rotation associated with the movement of neighbouring points. An index followed by a comma denotes partial differentiation with respect to space variables, while a superposed dot indicates the time derivative.

The constitutive equations are

$$\sigma_{kl} = \lambda e_{rr}\delta_{kl} + (2\mu + \kappa)e_{kl} + \kappa\varepsilon_{klm}(r_m - \varphi_m) + C_1\varphi_{r,r}\delta_{kl} + C_2\varphi_{k,l} + C_3\varphi_{l,k},$$

$$m_{kl} = \alpha\varphi_{r,r}\delta_{kl} + \beta\varphi_{k,l} + \gamma\varphi_{l,k} + C_1 e_{rr}\delta_{kl} + (C_2 + C_3)e_{kl} + (C_3 - C_2)\varepsilon_{klm}(r_m - \varphi_m), \tag{23}$$

where $e_{kl} = 1/2(u_{k.l} + u_{l,k})$ is the macrostrain tensor, λ, and μ are the Lamé elastic constants, κ is the Cosserat rotation modulus ($\kappa = 0$ corresponds to decoupling of the rotational and translational degrees of freedom, while $\kappa \to \infty$ corresponds to incompressibility), α, β, γ are the Cosserat rotation gradient moduli, and C_i, $i = 1,2,3$ are the chiral elastic constants associated with noncentrosymmetry. For $C_i = 0$, the isotropic micropolar elasticity constitutive laws are obtained, while for $\alpha = \beta = \gamma = \kappa = 0$, the classical isotropic linear elasticity case is retrieved. The internal energy must be nonnegative (the material is stable) and, therefore, the following restrictions on the micropolar elastic constants are obtained: $0 \leq 3\lambda + 2\mu + \kappa$, $0 \leq 2\mu + \kappa$, $0 \leq \kappa$, $0 \leq 3\alpha + \beta + \gamma$, $-\gamma \leq \beta \leq \gamma$, $0 \leq \gamma$ [Gauthier (1982); Lakes and Benedict (1982); Eringen (1966, 1968)].

The initial conditions attached to (22) are given by

$$u_i(x,y,z,0) = u_i^0(x,y,z), \quad \varphi_i(x,y,z,0) = 0, \quad i = 1,2,3,$$

$$m_{ij}(x,y,z,0) = 0, \quad \sigma_{ij}(x,y,z,0) = 0, \quad i = j \neq 3. \tag{24}$$

Eqs. (23) are similar in the form to equations of linear piezoelectricity. This correspondence can be useful to be used to define the Cosserat coefficients and the manner they are linked to the material itself.

The material is characterized by nine material constants, i.e. Lamé elastic constants λ and μ, Cosserat rotation modulus κ, Cosseratgg rotation gradient moduli α, β, γ, and chiral elastic constants C_i, $i = 1,2,3$.

Determination of Cosserat elastic constants can be achieved by the method of size effects for torsion and bending in the case of rods. The method consists in studying the variation of the rigidity divided by the square of the diameter with respect to the square of the diameter.

A more simple way to compute the material constants is to determine them directly from the expression of the potential energy of deformation per unit volume ψ

$$\psi = A_0 + A_{kl}\varepsilon_{kl} + \frac{1}{2}A_{klmn}\varepsilon_{kl}\varepsilon_{mn} + B_{kl}\varphi_{k,l} + \frac{1}{2}B_{klmn}\varphi_{k.l}\varphi_{m,n} + C_{klmn}\varepsilon_{kl}\varphi_{m,n}. \tag{25}$$

as

$$\begin{aligned} A_{kl} &= \frac{1}{2}\frac{\partial\psi}{\partial\varepsilon_{kl}}, \quad A_{klmn} = \frac{\partial^2\psi}{\partial\varepsilon_{kl}\partial\varepsilon_{mn}}, \\ B_{kl} &= \frac{1}{2}\frac{\partial\psi}{\partial\varphi_{k,l}} B_{klmn} = \frac{\partial^2\psi}{\partial\varphi_{k,l}\partial\varphi_{m,n}}, \quad C_{klmn} = \frac{\partial^2\psi}{\partial\varepsilon_{kl}\partial\varphi_{m,n}}, \end{aligned} \tag{26}$$

where $\varepsilon_{kl} = e_{kl} + \varepsilon_{klm}(r_m - \varphi_m)$.

Eringen (1968), Gauthier and Jahsman (1975), and Lakes (1995) presented some technical constants for $C_i = 0$in terms of physical insight, derived from the tensorial constants:

Young's modulus $E = \frac{(2\mu+\kappa)(3\lambda+2\mu+\kappa)}{2\lambda+2\mu+\kappa}$,

shear modulus $G = \frac{2\mu+\kappa}{2}$,

Poisson's ratio $\nu = \frac{\lambda}{2\lambda+2\mu+\kappa}$,

characteristic length for torsion $l_t = \sqrt{\frac{\beta+\gamma}{2\mu+\kappa}}$,

characteristic length for bending $l_b = \sqrt{\frac{\gamma}{2(2\mu+\kappa)}}$ (a slender bar with cross sectional area having the same order to l_b is stiffer than expected classically),

coupling number $N = \sqrt{\frac{\kappa}{2(\mu+\kappa)}} \leq 1$ (for $N = 1$ or $\kappa \to \infty$ i.e. incompressibility, the Cosserat theory is reduce to Mindlin and Tiersten theory (1962),

polar ratio $\psi = \frac{\beta+\gamma}{\alpha+\beta+\gamma}$.

Gauthier and Jahsmann (1975) have demonstrated that E and ν are determined from a tension test of rods as in the classical case, while cylindrical bending of a plate gives E and l_b. Size effect occurs in torsion, and the Cosserat constants G, l_t, N and ψ can be obtained from size effect data for torsion of rods of circular section. Bending of circular section rods of different size gives E, l_b, N.

The chiral coefficients are involved in the magnitude of couple stresses arising from chirality. Following Lakes (2001), the measurement of m_{zz} by a torque sensor in the compression of a glued slab gives $(C_1 + C_2 + C_3)$. The axial couple stress equation is $m_{zz} = (C_1 + C_2 + C_3)e$ where e is the strain. By measuring the moment due to m_{xx} in the side constraint by a torque sensor, we can determine C_1 via equation $m_{xx} = C_1 e$. Measurement of the shear force gives $(C_2 + C_3)$. The modulus κ can be determined in the lubrificated slab compression test by measurement of σ_{xy} by a shear force sensor via equation $\sigma_{xy} = -\kappa\varphi_z$.

Let us consider a cylindrical cube $r \leq R_2$ filled with conventional foam. The constitutive equations (23) of the foam are rewritten in cylindrical coordinates (Lakes and Benedict 1982)

$$[T_1] = \lambda e_{rr} + (2\mu + \kappa)[E_1] + C_1 \frac{1}{r}(r\varphi_r)_{,r} + \frac{1}{r}\varphi_{\theta,\theta} + \varphi_{z,z} + (C_2 + C_3)[\phi_1], \tag{27}$$

$$[T_2] = (\mu + \kappa)[E_2] + \mu[E_3] + C_2[\phi_2] + C_3[\phi_3],$$

$$[M_1] = \alpha \frac{1}{r}(r\varphi_r)_{,r} + \frac{1}{r}\varphi_{\theta,\theta} + \varphi_{z,z} + (\beta + \gamma)[\phi_1] + C_1\varepsilon_{ii} + (C_2 + C_3)[E_1],$$

$$[M_2] = \beta\left[\phi_2'\right] + \gamma\left[\phi_3'\right] + C_2[E_2] + C_3[E_3],$$

where

$$[T_1] = [\sigma_{rr}, \sigma_{\theta\theta}, \sigma_{zz}]^T, \quad [E_1] = [\varepsilon_{rr}, \varepsilon_{\theta\theta}, \varepsilon_{zz}]^T, \quad [\phi_1] = [\varphi_{rr}, \varphi_{\theta\theta}, \varphi_{zz}]^T,$$

$$[T_2] = [\sigma_{r\theta}, \sigma_{rz}, \sigma_{\theta r}, \sigma_{\theta z}, \sigma_{zr}, \sigma_{z\theta}]^T, \quad [E_2] = [\varepsilon_{r\theta}, \varepsilon_{rz}, \varepsilon_{\theta r}, \varepsilon_{\theta z}, \varepsilon_{zr}, \varepsilon_{z\theta}]^T,$$

$$[E_3] = [\varepsilon_{\theta r}, \varepsilon_{zr}, \varepsilon_{r\theta}, \varepsilon_{z\theta}, \varepsilon_{rz}, \varepsilon_{\theta z}]^T, \quad [\phi_2] = [-\frac{1}{r}\varphi_\theta, \varphi_{r,z}, \varphi_{\theta,r}, \varphi_{\theta,z}, \varphi_{z,r}, \phi_{z,\theta}]^T,$$

$$[\phi_3] = [\varphi_{\theta,r}, \varphi_{z,r}, -\frac{1}{r}\varphi_\theta, \varphi_{z,\theta}, \varphi_{r,z}, \varphi_{\theta,z}]^T,$$

$$[M_1] = [m_{rr}, m_{\theta\theta}, m_{zz}]^T, \quad [M_2] = [m_{r\theta}, m_{rz}, m_{\theta r}, m_{\theta z}, m_{zr}, m_{z\theta}]^T,$$

$$\left[\phi_2'\right] = [\frac{1}{r}\varphi_\theta, \varphi_{r,z}, \varphi_{\theta,r}, \varphi_{\theta,z}, \varphi_{z,r}, \phi_{z,\theta}]^T,$$

$$\left[\phi_3'\right] = [\varphi_{\theta,r}, \varphi_{z,r}, \frac{1}{r}\varphi_\theta, \varphi_{z,\theta}, \varphi_{r,z}, \varphi_{\theta,z}]^T.$$

The micropolar strains in terms of the displacements u and microrotations φ are given by

$$\varepsilon_{rr} = u_{r,r}, \quad \varepsilon_{\theta\theta} = \frac{1}{r}u_r, \quad \varepsilon_{zz} = u_{z,z}, \quad \varepsilon_{r\theta} = u_{\theta,r} - \varphi_z, \quad \varepsilon_{rz} = u_{z,r} + \varphi_\theta, \quad \varepsilon_{\theta z} = -\varphi_r,$$

$$\varepsilon_{\theta r} = -\frac{1}{r}u_\theta + \varphi_z, \quad \varepsilon_{zr} = u_{r,z} - \varphi_\theta, \quad \varepsilon_{z\theta} = u_{\theta,z} + \varphi_r.$$

The motion equations (22) become

$$\begin{aligned}
&\begin{bmatrix} \sigma_{rr,r} \\ \sigma_{r\theta,r} \\ \sigma_{rz,r} \end{bmatrix} + \frac{1}{r}\begin{bmatrix} \sigma_{rr} - \sigma_{\theta\theta} \\ \sigma_{r\theta} + \sigma_{\theta r} \\ \sigma_{rz} \end{bmatrix} = \rho \begin{bmatrix} \ddot{u}_r \\ \ddot{u}_\theta \\ \ddot{u}_z \end{bmatrix}, \\
&\begin{bmatrix} m_{rr,r} \\ m_{r\theta,r} \\ m_{rz,r} \end{bmatrix} + \frac{1}{r}\begin{bmatrix} m_{rr} - m_{\theta\theta} \\ m_{r\theta} + m_{\theta r} \\ m_{rz} \end{bmatrix} + \begin{bmatrix} \sigma_{\theta z} - \sigma_{z\theta} \\ \sigma_{zr} - \sigma_{rz} \\ \sigma_{r\theta} - \sigma_{\theta r} \end{bmatrix} = \rho j \begin{bmatrix} \ddot{\varphi}_r \\ \ddot{\varphi}_\theta \\ \varphi_z \end{bmatrix}.
\end{aligned} \tag{28}$$

The cylindrical cube is filled with conventional foam which has pores with average diameter around $900\mu m$ and a substantially isotropic distribution of the principal axis of the cells in the various directions. This foam has a positive Poisson's ratio By deforming it, we try to obtain initially deformed foams which can be auxetic or not. For example, Bezazi and Scarpa (2007) have obtained by manufacturing process foams with ν =0.25 at an initial compressive strain of 10%, which decreases sharply with the increase of compressive loading, to become slightly negative from 60 to 80% of tensile strain.

4 Transformed relations

An auxetic material with large absolute value of negative Poisson's ratio is difficult to realize. The highly negative Poisson's ratio material about $\nu = -10$ with extremely high permittivity is a good candidate for auxetic metamaterials. To obtain such a material, it is necessary to deform the foam (compression) virtually isotropically regardless of the deformation, nearly zero shear strain. An efficient auxetic metamaterial must allow the highest effective permittivity out of a given dielectric material.

We start to transform a cylindrical region filled with conventional foam into a cylindrical region filled with initial deformed foam.

The idea is to deform the cylindrical cube in the [111] direction, which is represented in Figure 1, by axis Xparallel to OD (diagonal of the cube) and normal to ABC. The deformation can be analyzed easily by considering the three sets of axes with the same origin O and described in Section 2:

- natural or stress-free configuration C_0 (position of a point P has coordinates $\xi_\mu(\mathrm{P})$),

- initially deformed equilibrium configuration $\tilde{C}$ (position of a point P has coordinates $X_A(\mathrm{P})$),

- present configuration $C(t)$, where t is the time (position of a point P has coordinates $x_i(\mathrm{P},t)$.

The set of axis (ξ_1,ξ_2,ξ_3) are parallel to three sides of the cylindrical cube, and the axes (X_1,X_2,X_3) are obtained from (ξ_1,ξ_2,ξ_3) with a 45^0 rotation around $\xi_3 \equiv X_3$. The axes (x_1,x_2,x_3) are obtained from (X_1,X_2,X_3) with a rotation around $X_2 \equiv x_2$ of an angle

$$\theta = \arcsin\frac{1}{\sqrt{3}}. \tag{29}$$

Figure 1a presents the cylindrical cube filled with conventional foam, and figure 1b, representation of the sets of axes (ξ_1,ξ_2,ξ_3), (X_1,X_2,X_3) and (x_1,x_2,x_3), used to study the cylindrical cube in a biaxially deformed state. The angle θ is defined in (29).

It can be easily shown that the transformation map from (ξ_1,ξ_2,ξ_3) to (X_1,X_2,X_3) is

$$X_1 = \frac{\xi_1+\xi_2+\xi_3}{\sqrt{3}}, \quad X_2 = \frac{-\xi_1+\xi_2}{\sqrt{2}}, \quad X_3 = \frac{-\xi_1-\xi_2+2\xi_3}{\sqrt{6}}. \tag{30}$$

The pores in the underformed cylindrical cube may be specified by three coordinates (ξ_1,ξ_2,ξ_3) which are integer or half-integer multiples of the constant a, the

only restriction being that $\xi_1+\xi_2+\xi_3$ must be an integer multiplier of a. Applying (30) we find that the corresponding coordinates in the (X_1,X_2,X_3) reference system are

$$X_1=\frac{la}{\sqrt{3}},\quad X_2=\frac{ma}{\sqrt{8}},\quad X_3=\frac{na}{\sqrt{24}}, \tag{31}$$

where l,m,n are integers, the only restrictions being that m and n must have the same parity

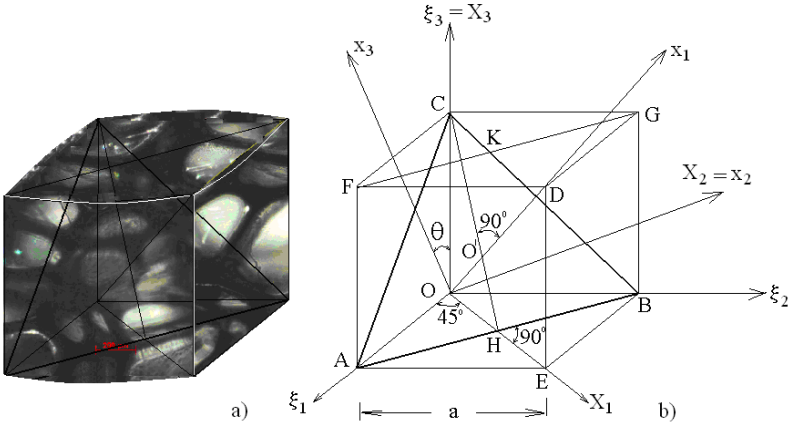

Figure 1: a) A cylindrical cube filled with conventional foam of side a; b) Representation of the sets of axes (ξ_1,ξ_2,ξ_3), (X_1,X_2,X_3) and (x_1,x_2,x_3).

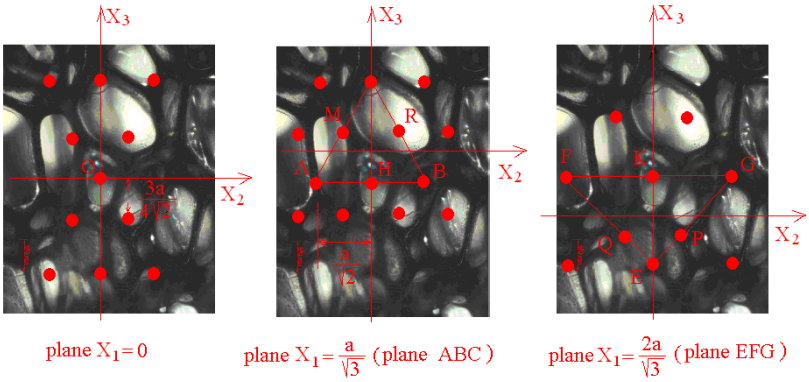

Figure 2: Representation of the cylindrical cube in (X_1,X_2,X_3) reference system.

Figure 2 shows a possible arrangement of pores into the cylindrical cube, as obtained from (31), for the plane $ABCx_1 = \frac{a}{\sqrt{3}}$ and the two neighboring planes $x_1 = 0$ and $x_1 = \frac{2a}{\sqrt{3}}$ of a central pore. Figure 2 shows all pores positions shown in Figure 1, except for the point D, which lies in the plane $x_1 = \frac{3a}{\sqrt{3}}$. Using (31) is it easy to represent the eight' nearest neighbors' of the central pore (say the pore at O).

In Figure 3 we show them schematically both in the (ξ_1, ξ_2, ξ_3) and (X_1, X_2, X_3) systems of axes. In the underformed cylindrical cube they are located at a distance $\frac{a}{\sqrt{2}}$ from O.

In the (x_1, x_2, x_3) system, a biaxial deformation in the [111] direction can be described by the transformation

$$x_1 = X_1(1+\varepsilon'), \quad x_2 = X_2(1+\varepsilon), \quad x_3 = X_3(1+\varepsilon), \tag{32}$$

where X_i are the coordonates of the pore positions in initial deformed state $\tilde{C}$.

The transformation (32) can be used to obtain the coordinates after the biaxial deformation, for twelve nearest neighbours shown in Figure 3. Alternatively, Figure 3 is used directly to read the coordinates, with the proviso that, in the equations of the planes, a becomes $a(1+\varepsilon')$ and, in the planes themselves, a becomes $a(1+\varepsilon)$.

Relations (30) and (32) allow transforming the foam in the configuration C_0 into foam with initial deformation in the configuration $\tilde{C}$. This conventional foam is characterized by the material constants given by (20).

Next, we couple the above transformation with a linear geometric transformation (1) applied to the foam in the configuration $\tilde{C}$. This transformation maps the cylindrical cube $r \leq R_2$ filled with initial deformed foam (auxetic or not) into the cylindrical shell $R_1 \leq r' \leq R_2$ filled with a new material. The transformation is given by

$$r' = R_1 + r\frac{R_2 - R_1}{R_2}, \quad 0 \leq \varphi \leq 2\pi, \quad \varphi' = \varphi, \quad z' = z, \tag{33}$$

where r', φ', z' are radially contracted cylindrical coordinates r, φ, z. The Cartesian basis (x_1, x_2, x_3) is defined as $x_1 = r\sin\theta\cos\varphi$, $x_2 = r\sin\theta\sin\varphi$, $x_3 = r\cos\theta$. The Jacobian of the transformation from cylindrical to stretched cylindrical coordinates is given by $J_{rr'} = \frac{\partial(r,\varphi,z)}{\partial(r',\varphi',z')}$.

This new material is an auxetic metamaterial characterized by material functions A'_{iMkN} given by

$$A'_{iMkN} = \frac{J^T_{rr'} \cdot \tilde{A}_{iMkN} \cdot J_{r'r}}{\det(J_{rr'})}, \tag{34}$$

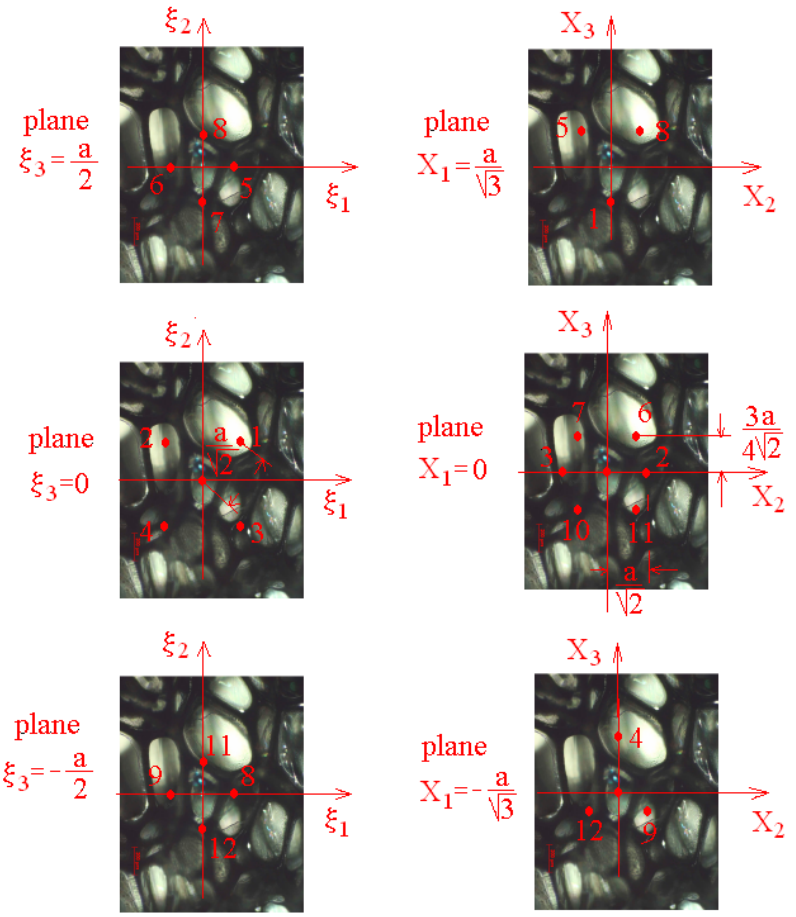

Figure 3: Representation of the twelve nearest neighbours (a) in the (ξ_1,ξ_2,ξ_3) system and b) in the (X_1,X_2,X_3) system.

where $\tilde{A}_{iMkN}$ are defined in (20)

$$\tilde{A}_{iMkN}=\left(\frac{X}{\xi}\right)^{-1}\frac{\partial X_M}{\partial \xi_\mu}\frac{\partial X_N}{\partial \xi_\nu}\tilde{\alpha}_{i\mu k\nu} \quad . \tag{35}$$

We are concentrated in next section to the properties of auxetic metamaterial. The interaction of meta-cells may be a way to understand this material. The auxetics gain its properties from its structure rather than directly from the composition. The meta-cells are much smaller in physical size than the wavelength. The material functions reflect the small scale anisotropy, heterogenity and large scale homo-

geneity. Metamaterials offer new propagation modes which can be explored as media for data exchange [Stevens (2013)] or resonators for the implementation of effective media metamaterials [Naqui, Martin (2014)]. New concepts in the area of hybrid metamaterials are presented by Sonkusale, Xu and Rout (2014).

5 Computation of the auxetic metamaterial functions

We derive general formulae for calculation the material functions. We adopt the Delsanto model (1992) in which the potential energy of deformation per unit volume ψ given by (26) equals the Born-Mayer ion-core repulsive energy written as

$$\psi = \frac{E}{\Omega}, \quad E = \tfrac{1}{2}\alpha_r \sum_R \exp(-\beta_r R), \tag{36}$$

where Ω is the cylindrical cube volume and α_r, β_r are the repulsive energy parameter and respectively the repulsive range parameter. The sum is extended to all the nearest neighbors which are meta-cells located at distances $R^{(n)}$. The material constants are determined from (26)

$$\begin{aligned} &A_{kl} = \frac{1}{2}\frac{\partial \psi}{\partial \varepsilon_{kl}}, \quad A_{klmn} = \frac{\partial^2 \psi}{\partial \varepsilon_{kl}\partial \varepsilon_{mn}}, \quad B_{kl} = \frac{1}{2}\frac{\partial \psi}{\partial \varphi_{k,l}}, \\ &B_{klmn} = \frac{\partial^2 \psi}{\partial \varphi_{k,l}\partial \varphi_{m,n}}, \quad C_{klmn} = \frac{\partial^2 \psi}{\partial \varepsilon_{kl}\partial \varphi_{m,n}}, \end{aligned} \tag{37}$$

where $\varepsilon_{kl} = e_{kl} + \varepsilon_{klm}(r_m - \varphi_m)$, and ψ given by (25)

$$\psi = A_0 + A_{kl}\varepsilon_{kl} + \frac{1}{2}A_{klmn}\varepsilon_{kl}\varepsilon_{mn} + B_{kl}\varphi_{k,l} + \frac{1}{2}B_{klmn}\varphi_{k.l}\varphi_{m,n} + C_{klmn}\varepsilon_{kl}\varphi_{m,n}. \tag{38}$$

Starting with (36)- (38), Delsanto proceeded to determine the elastic constants based on the formula

$$\frac{\partial}{\partial \varepsilon_{ij}} = \frac{1}{2}(X_i \frac{\partial}{\partial x_j} + X_j \frac{\partial}{\partial x_i}), \quad \varepsilon_{kl} = e_{kl} + \varepsilon_{klm}(r_m - \varphi_m). \tag{39}$$

In (39) X_i are the coordinates corresponding to configuration $\tilde{C}$, and x_i are the final coordinates. It is important to note that, in applying of (39) the coordinates X_i are constants since they refer to a predefined initial state. Using (39) it is straightforward to prove that the following relation holds for a differentiable function $f(r)$,

$$\left(\frac{\partial f(r)}{\partial \varepsilon_{kl}}\right)_{r=R} = \frac{1}{R^2}[Rf'(R) - f(R)]Y_{kl} + \frac{1}{2}f(R)Z_{kl}, \tag{40}$$

$$\left(\frac{\partial^2 f(r)}{\partial\varepsilon_{kl}\partial\varepsilon_{ij}}\right)_{r=R} = \frac{1}{R^3}[Rf''(R) - f'(R)]Y_{ijkl} + \frac{1}{4R}f'(R)Z_{ijkl}, \tag{41}$$

$$\left(\frac{\partial f(r)}{\partial\varphi_{k,l}}\right)_{r=R} = \frac{1}{R^3}[Rf''(R) - f'(R)]Y_{kl} + \frac{1}{4R}f'(R)Z_{kl}, \tag{42}$$

$$\left(\frac{\partial^2 f(r)}{\partial\varphi_{k,l}\partial\varphi_{m,n}}\right)_{r=R} = \frac{1}{R^4}[R^2 f''(R) - f''(R)]Y_{klmn} + \frac{1}{4R^2}f''(R)Z_{klmn}, \tag{43}$$

where

$$Y_{kl} = X_k X_l, \quad Y_{ijkl} = X_i X_j X_k X_l, \tag{44}$$

$$Z_{kl} = X_i X_k \delta_{il} + X_j X_l \delta_{jk}, \quad Z_{ijkl} = X_i X_k \delta_{jl} + X_i X_l \delta_{jk} + X_j X_l \delta_{ik} + X_j X_k \delta_{il}, \tag{45}$$

$$R = \sqrt{X_1^2 + X_2^2 + X_3^2}. \tag{46}$$

From (39)-(43) it then follows that

$$\begin{aligned} &A_{kl} = a_{kl} - a'_{kl}, \quad A_{klmn} = b_{klmn} - b'_{klmn}, \quad B_{kl} = c_{kl} - c'_{kl}, \\ &B_{klmn} = d_{klmn} - d'_{klmn}, \quad C_{klmn} = e_{klmn} - e'_{klmn}, \end{aligned} \tag{47}$$

where

$$a_{kl} = \sum_n f^{(n)} Y_{kl}^{(n)}, \quad a'_{kl} = \sum_n g^{(n)} Z_{kl}^{(n)}, \tag{48}$$

$$b_{ijkl} = \sum_n f^{(n)} Y_{ijkl}^{(n)}, \quad b'_{ijkl} = \sum_n g^{(n)} Z_{ijkl}^{(n)}, \tag{49}$$

$$c_{kl} = \sum_n (f^{(n)} + g^{(n)}) Y_{kl}^{(n)}, \quad c'_{kl} = \sum_n (f^{(n)} + g^{(n)}) Z_{kl}^{(n)}, \tag{50}$$

$$d_{ijkl} = \sum_n (f^{(n)} + g^{(n)}) f^{(n)} Y_{ijkl}^{(n)}, \quad d'_{ijkl} = \sum_n (f^{(n)} + g^{(n)}) g^{(n)} Z_{ijkl}^{(n)}, \tag{51}$$

$$e_{ijkl} = \sum_n (f^{(n)} + g^{(n)}) Y_{ijkl}^{(n)}, \quad e'_{ijkl} = \sum_n (f^{(n)} + g^{(n)}) Z_{ijkl}^{(n)}, \tag{52}$$

$$f^{(n)} = f(R^{(n)}) = 4g^{(n)} \left(1 + \frac{\beta R^{(n)}}{(R^{(n)})^2}\right), \tag{53}$$

$$g^{(n)} = g(R^{(n)}) = \frac{K}{R^{(n)}} \exp(-\beta R^{(n)}), \quad K = \frac{\alpha\beta}{8\Omega}. \tag{54}$$

Quantities $Y^{(n)}$, $Z^{(n)}$ and $R^{(n)}$ are calculated for the th nearest neighbour. Further, we present in Figure 4 the variation of the Lamé functions, λ (black) and μ (red) with respect to the strain. The Lamé functions were evaluated for strains between

-10% and 10%. This figure raises some questions. If consider the linear elasticity, $\lambda = \frac{E\nu}{(1-\nu)(1+\nu)}$ is related to the bulk modulus; it can be negative in principle, and the shear modulus $\mu = \frac{E}{2(1+\nu)}$ must be positive. The $(1+\nu)$factor reduces to zero for $\nu = -1$. For $\nu \to -\infty$, $\lambda, \mu \to 0$ the material seems to weaken in terms of these properties. Figure 4 shows that the shear modulus can be negative for certain strain.

Let take an arbitrary strain in Figure 4, say -0.055. Our computations show that the Poisson's ratio is -12, and the Lamé functions have values λ =0.2517 and $\mu = -0.136$, respectively. These values correspond to $E = 3$GPA. The strange behavior of the Lamé functions shown in figure 4 can receive an explanation.

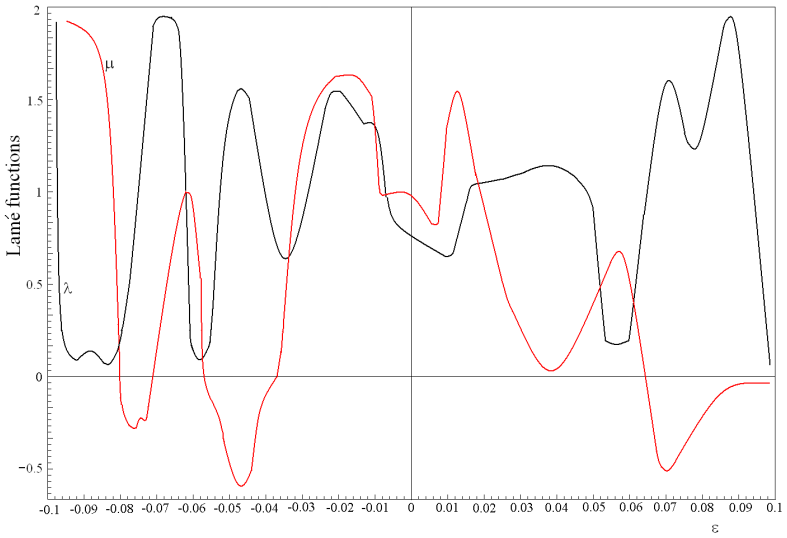

Figure 4: Plots of the Lamé function λ (black) and μ (red) in the (x_1, x_2, x_3) system as a function of the strain. The units are 1 GPa.

Caddock and Evans (1989) have investigated auxetic microporous polymeric materials and obtained expanded auxetic forms with Poisson's ratio larger in absolute value than -12. They explain the large Poisson's ratio by complex microstructure of the material characterised by nodules interconnected by fibrils. The dominant deformation mechanism for significant auxetic behavior is done by the nodule translation through hinging of the fibrils.

Kinloch and Young (1999) have observed a new phenomenon which appears during deformation of microporous polymeric materials. It comes the *crazing phenomenon* which is a failure mode met at the bulk polymers. During predominant

uniaxial tensile loading, the bulk forms denser ligaments (or fibrils) while preserving its continuity.

Hence, the behavior of the Lamé functions in figure 4 can be explained through the *crazing phenomenon.* The cracks are bridging the pores by such fibrils of about 10^{-10}m . This phenomenon is an important mechanism which works to the benefit of the metamaterial. Also, such fibres play an important role for energy dissipation in the auxetic metamaterial.

The auxetic material does not break at macro level; contrary have intrinsic porosity with fibres in order to achieve a large negative Poisson's ratio. This material needs fibres to allow pores to behave as hinges to flex, or nodules to spread out and so on. The material needs space to allow meta-cells to behave as hinges to flex, or nodules to spread out and so on. On the optimization of microstructures using the material design, see Li et al. (2006).

6 Seismic cloaking

Buildings and other structures can be protected from earthquakes by surrounding them with cloaking structures made of auxetic metamaterial. The cloaking structures can effectively convert the destructive seismic waves into a different type of wave whose intensity dissipates quickly.

For seismic cloak we choose an auxetic metamaterial with Poisson's ratio equals -10 obtained for a strain equals -0.08. The Lame functions are the values λ =0.1731 and $\mu = -0.0952$. The structure of auxetic metamaterial is atomic and the arrangement of meta-cells is about 10^{-10}m.

Let us consider a building foundation of height$l$, and the impulsive source (a seismic weight drop source) acting on the ground surface at 300 m from the foundation (Figure 5).

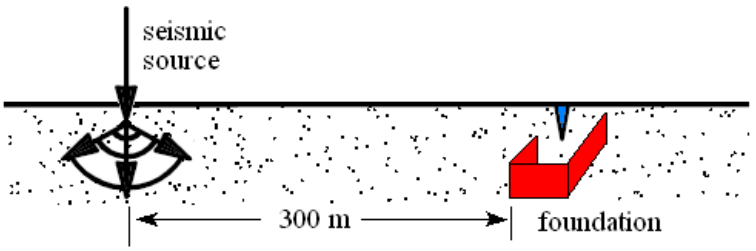

Figure 5: The seismic source and the foundation.

Our idea is to hide the foundation with a cloak whose function is to deflect the rays that would have struck the foundation, guide them around it, and return them to their original paths.

The cloak is composed by a number of Mcylindrical shells $R_1 \leq r' \leq R_2$, of length l, arranged on a circle of radius R. The cloak is placed in the ground around the structure in the plane of lower base of the foundation. The boundary of V which encloses the foundation is denoted by S, and p is the distance from one shell structure to the next one. The cloak and the cross section are shown in Figure 6a, b. The projection of foundation on the circle's plane is shown in the middle of the circle in Figure 6b.

The seismic invisibility conjures to the destructive interference, which is the essence of the Stokes's explanation [Stokes (1868)] for Leslie's experiment [Leslie (1821)]. In this experiment, the audibility of a bell ringing in a partly exhausted bell jar is diminished by the introduction of hydrogen [Williams (1984)]. As in seismic cloaking, the waves would not see the object and largely pass around it.

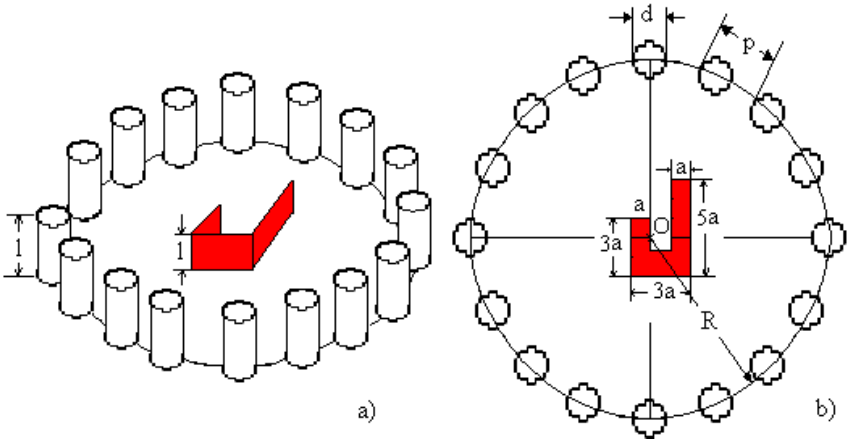

Figure 6: Seismic cloak structure. a) arrangement of M cylindrical shells on a circle enclosing the foundation. b) cross section through the cloak.

In order to illustrate the efficiency of the proposed seismic invisibility cloak, we have computed the surface wave field ϕ inside the cloak. The wave field is evaluated for a seismic source situated at 300 m from the foundation and 30 m depth (see Figure 7). Any waves inside V have the potential ϕ which verifies the equation

$$\frac{\partial^2 \phi}{\partial t^2} - c_S^2 \nabla^2 \phi = 0, \tag{55}$$

With c_S the velocity of S seismic waves $c_S = \sqrt{\frac{\mu}{\rho}}$, with μ the Lamé constant and ρ the density of the soil. The selection of the free space Green function G is made from the Kirchhoff's theorem

$$G = \frac{\delta(t - \frac{r}{c})}{(4\pi c^2 r)}, \quad r = |x - y|, \tag{56}$$

under the constraint that

$$\frac{\partial^2 G}{\partial t^2} - c_S^2 \nabla^2 G = \delta(x - y, t - \tau), \tag{57}$$

is valid for x and y lying within V. By integrating (55) and (57) we obtain the interior wave field ϕ inside the cloak

$$\phi = -c_S^2 \int_S \left\{ G \frac{\partial \phi}{\partial n} - \phi \frac{\partial G}{\partial n} \right\} \mathrm{d}S\mathrm{d}r, \tag{58}$$

Where n the normal to that surface leading into the volume V containing the building. The integral (58) is evaluated for a =1 M, l =1.5 M, R =6 M, d =0.355 and p =2.355. After computing the integral (58) is $\phi = 3.5 \times 10^{-4}$. This result shows that the surface integral (58) almost vanishes within V.

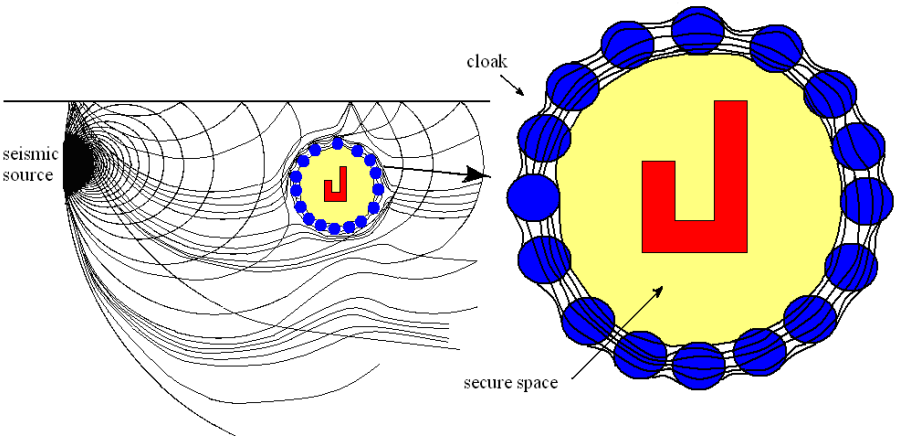

Figure 7: A 2D cross section of the ray trajectories in the cloak diverted within the arrangement of shells. The secure foundation is hidden inside the secure space of the cloak.

Since geometric transformation establishes a one-to-one correspondence between spatial geometries and auxetic medium, invisibility can be visualized in terms of

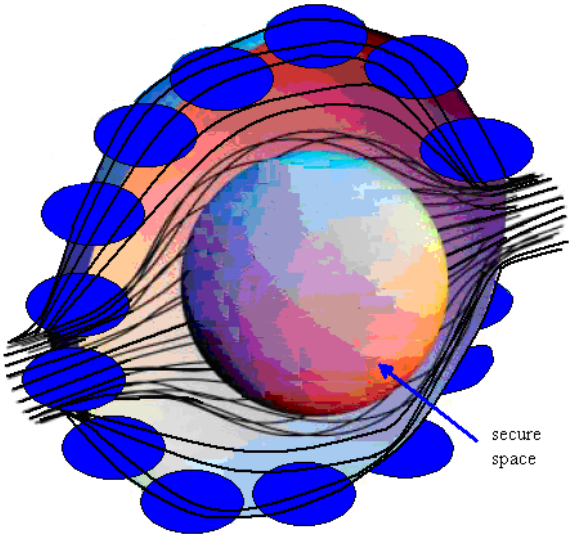

Figure 8: A 3D view of the cloak.

virtual geometries. Therefore, we have explained the main ideas of this paper in terms of pictures.

Figure 7 shows the isolated cloak from the region situated outside of V. No rays can get into the secure volume, nor can any rays get out. Any ray attempting to penetrate the secure space is smoothly guided around by the cloak in order to travel in the same direction as if it had passed through the empty volume of space. The rays field ϕ generated by the seismic source essentially follows the Poynting vector and it is smoothly confined on the cloak boundary region. The cloak is seismically isolated and the surface waves are not detectable by observers inside the cloak because the amplitudes on the boundary vanish.

A 3D view of the cloak is shown in Figure 8. The profile of the cloak is highly anisotropic within the arrangement of the cylindrical shells and isotropic outside it.

7 Conclusions

The primary aim of this paper is to discuss the auxetic metamaterials controlled by geometric transformations. These transformations are derived from the theory of small (infinitesimal) elastic deformation superimposed on finite elastic deformations. Using this theory, a cylindrical region filled with initial deformed foam is transformed through deformation into a cylindrical shell region filled with auxetic metamaterial. For calculation of the material constants, the Delsanto model

is adopted. In this model, the potential energy of deformation per unit volume is given the Born-Mayer ion-core repulsive energy. The Lamé functions behavior is explained through the *crazing phenomenon* which is a failure mode met at the bulk polymers.

We show that the auxetic metamaterial is capable to create barriers that would cloak buildings from the seismic waves of earthquakes by diverting the seismical energy around building and foundations. The seismic waves traveling toward the building are directed around the building and leave the building unscathed. The auxetic cylinders arrangement around the foundation manipulates the seismic waves in order to destructively interferes and to counteract the effects of seismic waves. The cloak can effectively convert the destructive seismic waves into a different type of wave whose intensity dissipates quickly.

Acknowledgement: The authors gratefully acknowledge the financial support of the National Authority for Scientific Research ANCS/UEFISCDI through the through the project PN-II-ID-PCE-2012-4-0023, Contract nr.3/2013. The authors acknowledge the similar and equal contributions to this article.

References

Baughman, R. H. (2003): Avoidung the shrink. *Nature* 425.

Bezazi, A.; Scarpa, F. (2007): Mechanical behaviour of conventional and negative Poisson's ratio thermoplastic polyurethane foams under compressive cyclic loading. *International Journal of Fatique,* vol. 29, pp. 922–930

Bradford, M. A.; Pi, Y.-L. (2012): Nonlinear elastic-plastic analysis of composite members of high-strenght steel and geopolymer concrete. *CMES: Computer Modeling in Engineering & Sciences*, vol. 89, no. 5, pp. 389-416.

Brun, M.; Guenneau, S.; Movchan, A. B. (2009): Achieving control of in-plane elastic waves. *Applied Physics Letters,* vol. 94, 061903.

Bückmann, T.; Stenger, N.; Kadic, M.; Kaschke, J.; Frölich, A.; Kennerknecht, T.; Eberl, T.; Thiel, M.; Wegener, M. (2012): Tailored 3D mechanical metamaterials made by dip-in direct-laser-writing optical lithography. *Adv. Mater.*, vol. 24, pp. 2710-2714.

Baughman, R. H., Galvao, D. S. (1993): Crystalline network with unusual predicted mechanical and thermal properties. *Nature,* vol. 365, pp. 735-737.

Caddock, B. D.; Evans, K. E. (1989): Microporous materials with negative Poisson's ratio. I. Microstructure and mechanical properties. *Journal of Physics D:Appled Physics,* vol. 22, 1877.

Cipolla, J. L.; Gokhale, N. H. J.; Norris, A. N. (2010): Generalized transformation acoustics for material design. *Journal of the Acoustical Society of America,* vol. 128.

Cipolla, J. L.; Gokhale, N. H. J.; Norris, A. N. (2012): Special transformations for pentamode acoustic cloaking. *J. Acoust. Soc. Am.,* vol. 132, no. 4, pp. 2932-2941.

Chang, Z.; Hu, J.; Hu, G.-K. (2010): Transformation method and wave control. *Acta Mech. Sin.*, vol. 26, pp. 889-898.

Chiroiu, V.; Brişan, C.; Popescu, M. A.; Girip, I.; Munteanu, L. (2013): On the sonic composites without/with defects. *Journal of Applied Physics,* vol. 114, 164909.

Chiroiu, V.; Munteanu, L.; Ioan, R.; Moşneguţu, V. (2014): On the seismic cloaking. *Romanian Journal of Acoustics and Vibration*, vol. 11, no. 1, pp. 31-34.

Choudhury, B.; Iha, R. M. (2013): A review of metamaterial invisibility cloaks. *CMC: Computers, Materials& Continua,* vol. 33, no .3, pp. 275-308.

Cosserat. E.; Cosserat, F. (1909): Theorie des Corps Deformables (Hermann et Fills, Paris).

Cummer, S. A.; Popa, B. L.; Schurig, D.; Smith, D. R.; Pendry, J.; Rahm, M.; Starr, A. (2008): Scattering theory derivation of a 3D acoustic cloaking shell. *Physical Review Letters,* vol. 100, 024301.

Cummer, S. A.; Schurig, D. (2007): One path to acoustic cloaking. *New Journal of Physics,* vol. 9, pp. 45.

Delsanto, P. P.; Provenzano, V.; Uberall, H. (1992): Coherency strain effects in metallic bilayers. *J. Phys.: Condens. Matter*, vol. 4, pp. 3915-3928.

Donescu, St.; Chiroiu, V.; Munteanu, L. (2009): On the Young's modulus of a auxetic composite structure. *Mechanics Research Communications,* vol. 36, pp. 294–301.

Dupont, G.; Farhat, M.; Diatta, A.; Guenneau, S.; Enoch, S. (2011): Numerical analysis of three-dimensional acoustic cloaks and carpets. *Wave Motion,* vol. 48, no. 6, pp. 483–496.

Eringen, A. C. (1966): Linear Theory of Micropolar Elasticity. *Journal of Mathematics and Mechanics,* vol. 15, pp. 909–924.

Eringen, A. C. (1968): *Theory of micropolar elasticity*, in Fracture (ed. R. Liebowitz) 2, Academic Press, pp. 621–729.

Farhat, M.; Enoch, S.; Guenneau, S.; Movchan, A. B. (2009): *Cloaking bending waves propagating in thin elastic plates*, Phys. Rev. B 79, 033102, 2009.

Gauthier, R. D. (1982): *Experimental investigations on micropolar media* in: Mechanics of Micropolar Media, CISM Courses and lectures, edited by O. Brulin and R.K.T. Hsieh, World scientific, pp. 395-463.

Guenneau, S.; McPhedran, R. C.; Enoch, S.; Movchan, A. B.; Farhat, M.; Nicorovici, N. A. (2011): The colours of cloaks. *Journal of Optics,* vol. 13, no. 2, 024014.

Hirsekorn, M.; Delsanto, P. P.; Batra, N. K.; Matic, P. (2004): Modelling and simulation of acoustic wave propagation in locally resonant sonic materials. *Ultrasonics,* vol. 42, pp. 231–235.

Kadic, M.; Bückmann, T.; Stenger, N.; Thiel, M.; Wegener, M. (2012): On the practicability of pentamode mechanical metamaterials. *Appl. Phys. Lett.,* vol. 100, 191901.

Kinloch, A. J.; Young, R. J. (1999): Fracture Behavior of Polymers, Elsevier Applied Science, Essex 1983; E.K.Gamstedt, R.Talrega, Fatigue damage mechanisms in unidirectional carbon-fibre-reinforced plastics. *J. Mater. Sci.,* vol. 34, 2535.

Lakes, R. S. (1986): Experimental microelasticity of two porous solids. *Int. J. Solids Struct.* vol. 22, pp. 55–63.

Lakes, R. S. (1987): Foam structures with a negative Poisson's ratio. *Science,* vol. 235, pp. 1038–1040.

Lakes, R. S. (1991): Experimental micro mechanics methods for conventional and negative Poisson's ratio cellular solids as Cosserat continua. *J. Eng. Mater. Technol.*, vol. 113, pp. 148–155.

Lakes, R. S.; Elms, K. (1993): Indentability of conventional and negative Poisson's ratio foams. *Journal Composite Materials,* vol. 27, pp. 1193-1202.

Lakes, R. S.; Benedict, R. L. (1982): Noncentrosymmetry in micropolar elasticity. *Int. J. Engng. Sci*. vol. 20, no. 10, pp. 1161-1167 .

Lakes, R. (1995): Experimental methods for study of Cosserat elastic solids and other generalized elastic continua in Continuum models for materials with microstructure. ed. H.Muhlhaus, J.Wiley, N.Y.,Ch1, 1-22.

Lakes, R. (2001): Elastic and viscoelastic behavior of chiral materials. *Int. J. of mechanics Sciences*, vol. 43, pp. 1579-1589.

Leonhardt, U. (2006): Optical conformal mapping. *Science,* vol. 312, pp. 1777–1780.

Leslie, J. (1821): On sounds excited in hydrogen gas. *Trans. Camb. Phil . Soc.*, vol. 1, no. 2, pp. 267-268.

Li, D. S.; Saheli, G.; Khaleel, M.; Garmestani, H. (2006): Microstructure opti-

mization in fuel cell electrodes using materials design, *CMC: Computers, Materials & Continua*, vol. 4, pp. 31-42.

Mindlin, D. (1965): Stress functions for a Cosserat continuum *International Journal of Solids and Structures.* vol. 1, pp. 265–271.

Mindlin, R. D.; Tiersten, H. F. (1962): Effect of couple stresses in linear elasticity. *Arch. Rational Mech. Analy,* vol. 11, pp. 415-448.

Milton, G. W.; Cherkaev, A. V. (1995): Which elasticity tensors are realizable? *J. Eng. Mater. Technol.,* vol. 117, pp. 483–493.

Milton, G. W.; Nicorovici, N. A. (2006): On the cloaking effects associated with anomalous localized resonance. *Proc. Roy. Soc. A,* vol. 462, pp. 3027–3059.

Milton, G. W.; Briane, M.; Willis, J. R. (2006): On cloaking for elasticity and physical equations with a transformation invariant form. *New Journal of Physics,* vol. 8, 248.

Milton, G. W. (2007): New metamaterials with macroscopic behavior outside that of continuum elastodynamics. *New Journal of Physics,* vol. 9, pp. 359– 372.

Milton, G. W. (2013): Adaptable nonlinear bimode metamaterials using rigid bars, pivots, and actuators. *J. Mech. Phys. Solids,* 611543–1560

Munteanu, L.; Chiroiu, V.; Donescu, St.; Brişan, C. (2014): A new class of sonic composites. *Journal of Applied Physics*, vol. 115, 104904-1-11.

Munteanu, L. (2012): *Nanocomposites.* Publishing House of the Romanian Academy Bucharest.

Munteanu, L.; Chiroiu, V. (2010): On the dynamics of locally resonant sonic composites. *European Journal of Mechanics-A/Solids,* vol. 29, no. 5, pp. 871–878.

Munteanu, L.; Chiroiu, V. (2011): On the three-dimensional spherical acoustic cloaking. *New Journal of Physics*, vol. 13, no. 8, pp. 1–12

Munteanu, L.; Brişan, C.; Donescu, St.; Chiroiu, V. (2012): On the compression viewed as a geometric transformation. *CMC: Computers, Materials & Continua*, vol. 31, no. 2, pp. 127–146.

Naqui, J.; Martin, F. (2014): Some applications of metamaterials resonators based on symmetry properties. *CMC: Computers, Materials & Continua*, vol. 39, no. 3, pp. 267-288.

Narayan, S.; Latha, S.; Jha, R. M. (2013): EM analysis of metamaterial based radar absorbing structure (RAS) for millimeter wave applications. *CMC: Computers, Materials & Continua,* vol. 34, no. 2, pp. 131-142.

Nicorovici, N. A.; McPhedran, R. C.; Milton, G. W. (1994): Optical and di-

electric properties of partially resonant composites. *Phys. Rev. B,* vol. 490, pp. 8479–8482.

Norris, A. N. (2008): Acoustic cloaking theory. *Proc. R. Soc. London, Ser. A,* vol. 464 pp. 2411-2434.

Norris, A. N.; Shuvalov, A. L. (2011): Elastic cloaking theory. *Wave Motion,* vol. 48, no. 6, pp. 525-538.

Novitsky, A.; Qiu, C.-W.; Zouhdi, S. (2009): Transformation-based spherical cloaks designed by an implicit transformation-independent mthod: theory and optimization. *New Journal of Physics,* vol. 11, 113001.

Parnell, W. J. (2012): Nonlinear pre-stress for cloaking from antiplane elastic waves. *Proceedings of the Royal Society A mathematical, Physical & Engineering Sciences,* vol. 468(2138)

Parnell, W. J.; Norris, A. N.; Shearer, T. (2012): Employing pre-stress to generate finite cloaks for antiplane elastic waves. *Appl. Phys. Lett*., vol. 100, no. 17.

Pendry, J. B.; Shurig, D.; Smith, D. R. (2006): Controlling electromagnetic fields. *Science*, vol. 312, pp. 1780–1782

Qiu, C. W.; Hu, L.; Zhang, B.; Wu, B. I.;, Johnson, S. G.; Joannopoulos, J. D. (2009): Spherical cloaking using nonlinear transformations for improved segmentation into concentric isotropic coatings. *Optics Express,* vol. 17, no. 16, pp. 13467–13478.

Scandrett, C. L.; Boisvert, J. E.; Howarth, T. R. (2010): Acoustic cloaking using layered pentamode materials. *J. Acoust. Soc. Am*., vol. 127, no. 5, pp. 2856–2864.

Scarpa, F.; Giacomin, J.; Zhang, Y.; Pastorino, P. (2005): Mechanical Performance of Auxetic Polyurethane foam for antivibration glove applications. *Cellular Polymer,* vol. 24, pp. 253-268.

Schurig, D.; Pendry, B.; Smith, D. R. (2006): Calculation of material properties and ray tracing in transformation media. *Opt. Express*, vol. 14, pp. 9794-9804.

Sonkusale, S. R.; Xu, W.; Rout, S. (2014): Active metamaterials for modulation and detection. *CMC: Computers, Materials & Continua*, vol. 39, no. 3, pp. 301-315.

Stenger, N.; Wilhelm, M.; Wegener, M. (2012): Experiments on Elastic Cloaking in Thin Plates. *Phys. Rev.Lett*., vol. 108, 014301.

Stevens, C. J. (2013): Power transfer via matematerials. *CMC: Computers, Materials & Continua*, vol. 33, no. 1, pp. 1-18.

Stokes, G. (1868): On the communication of vibrations from a vibrating body to a

surrounding gas. *Phil. trans. R. Soc. Lond.*, vol. 158, 447.

Torrent, D.; Sánchez-Dehesa, J. (2008): Anisotropic mass density by two-dimensional acoustic metamaterials. *New J. Phys.*, vol. 10, 023004.

Toupin, R. A.; Bernstein, B. (1961): Sound waves in deformed perfectly elastic materials Acoustoelastic effect. *J. Acoust. Soc. Am.*, vol. 33, no. 2, pp. 216-225.

Williams, F. (1984): Antisound, *Proc. R. Soc Lond. A,* vol. 395, pp. 63-88.

Zolla, F.; Guenneau, S.; Nicolet, A.; Pendry, J. B. (2007): Electromagnetic analysis of cylindrical invisibility cloaks and the mirage effect. *Opt. Letters,* vol. 32, pp. 1069–1071.